



Modelling of pyrocarbon chemical vapor infiltration

Nicolas Reuge, Gerard L. Vignoles, H. Le Poche, Francis Langlais

► To cite this version:

Nicolas Reuge, Gerard L. Vignoles, H. Le Poche, Francis Langlais. Modelling of pyrocarbon chemical vapor infiltration. *Advances in Science and Technology*, 2002, 36, pp.259-266. hal-00337422

HAL Id: hal-00337422

<https://hal.science/hal-00337422>

Submitted on 12 Dec 2008

HAL is a multi-disciplinary open access archive for the deposit and dissemination of scientific research documents, whether they are published or not. The documents may come from teaching and research institutions in France or abroad, or from public or private research centers.

L'archive ouverte pluridisciplinaire **HAL**, est destinée au dépôt et à la diffusion de documents scientifiques de niveau recherche, publiés ou non, émanant des établissements d'enseignement et de recherche français ou étrangers, des laboratoires publics ou privés.

Proc. 3rd Forum on New Materials vol. 1 :
Computational Modelling and simulation of Materials II,
P. Vicenzini and P. A. Glasow eds.
p. 259-266,
Techna, Faenza, Italy (2002).

MODELLING OF PYROCARBON CHEMICAL VAPOR INFILTRATION

Nicolas Reuge,

Gerard L. Vignoles*

H. Le Poche

F. Langlais

Laboratoire des Composites ThermoStructuraux
(UMR 5801 CNRS-SNECMA-CEA-UBI)
3, Allée La Boétie, Domaine Universitaire, F33600 PESSAC, France
Fax (00 33) 5 56 84 12 25
E-mail : reuge@free.fr , vinhola@lcts.u-bordeaux.fr

* *To whom correspondence should be addressed*

MODELLING OF PYROCARBON CHEMICAL VAPOR INFILTRATION

Nicolas REUGE, Gerard L. VIGNOLES, Hélène Le POCHE, Francis LANGLAIS

LCTS : Laboratoire des Composites ThermoStructuraux
(UMR 5801 CNRS-SNECMA-CEA-Université Bordeaux 1)
3, Allée La Boétie, Domaine Universitaire, F33600 PESSAC, France
e-mail: reuge@free.fr,{vinhola,langlais}@lcts.u-bordeaux.fr

The chemical vapor infiltration (CVI) of pyrocarbon is used to produce carbon matrix of C/C composites. This process involves complex physico-chemical phenomena such as the transport of gas mixtures (hydrocarbons and hydrogen) in the reactor and inside the fibrous preform, chemical reactions (pyrolysis and deposition), and the structural evolution of the preform. A global modelling approach has been developed for isobaric CVI. The most difficult point is to find a realistic chemical model for pyrocarbon deposition chemistry, simple enough to be implemented in a 2D or 3D fluid dynamics code. Such a model is proposed in this study, featuring a group of light species leading to smooth laminar pyrocarbon, a group of heavier species (polycyclic hydrocarbons) leading to rough laminar pyrocarbon, and associated homogeneous and heterogeneous reaction kinetics. This model has been developed and validated according to results of pyrocarbon CVD experiments from propane, and isothermal, isobaric CVI in a 1D model porous medium made of compact stacks of 100 μm diameter filaments.

1. INTRODUCTION

Carbon/carbon (C/C) composite materials are used in high-temperature applications, such as rocket nozzle, heat shields, airplane braking, and furnace components. For a high thermal and mechanical quality, CVI-processed pieces are preferred. CVI¹ stands for Chemical Vapor Infiltration, a process derived from CVD (chemical vapor deposition), in which a preform made of carbon fibers is densified by a pyrocarbon (*pyC*) deposit originated in the cracking of gaseous hydrocarbons, usually at high temperatures (ca. 1000–1300 K) and low pressures. This process allows the fabrication of complex pieces without damaging the carbon fibers and results in excellent mechanical and thermal properties.

Hydrocarbon pyrolysis is known to lead to various nanotextural forms of pyrocarbon in the context of CVD and/or CVI^{2,3}. Among them, two varieties, referred to as Rough Laminar (RL) and Smooth Laminar (SL) because of their appearances when imaged by Polarized Light Optical Microscopy (PLOM), differ by their degree of structural anisot-

ropy, and have distinct mechanical and optical properties. Moreover, only the RL form is graphitizable by high-temperature post-treatment^{3,4}. A key issue in pyC CVD/CVI is the control of the deposit nanostructure during processing. It has been shown⁵⁻⁷ that processing parameters such as temperature, pressure, and composition ratios are important for this.

Another crucial issue in C/C composite quality monitoring is the precise knowledge of the deposition kinetics as a function of the process parameters : temperature, pressure, residence time, gas composition, and surface-to-volume ratio S/V. Numerous experimental studies⁸⁻¹⁵ have been devoted to the determination of kinetic laws in various physico-chemical conditions and reactor configurations, either in CVD (plain substrate, low S/V ratio), or in CVI (porous substrate, high S/V ratio). All of them have tried to identify some “ultimate precursor” of pyC, either light, aliphatic species, or heavy aromatic compounds such as PAHs (Polycyclic Aromatic Hydrocarbons). It has been proved, from mass spectroscopy¹⁶, gas chromatography^{17,18} and FT-IR^{19,20} measurements of the gas-phase composition, that the hydrocarbon pyrolysis follows a long chain of homogeneous reactions, starting from light species and leading to large PAHs, in a so-called “maturation” process. The pyrocarbon deposits come from both light and heavy hydrocarbons, and their nanostructure undergoes transitions from SL to RL and vice-versa when the residence time increases^{21,22}.

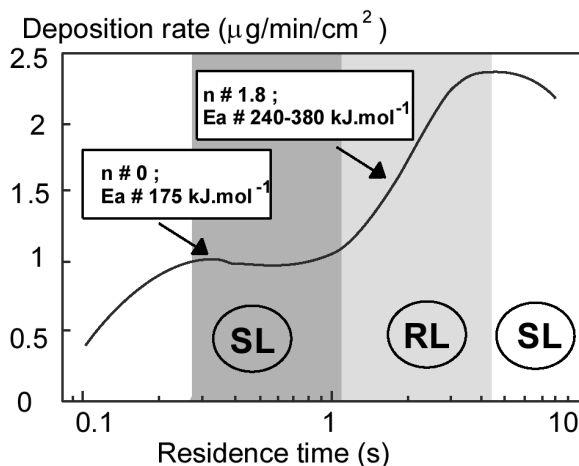


FIGURE 1
Deposit rate vs. residence time. Precursor : propane, $T = 950^{\circ}\text{C}$, $P = 2 \text{ kPa}$.

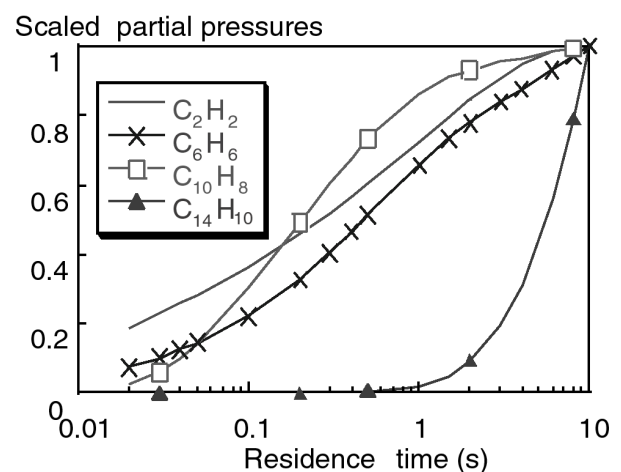


FIGURE 2
Scaled partial pressures of various species from computations (ref. [23]).

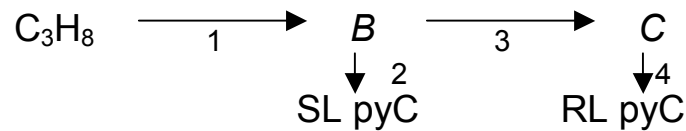
A kinetic modeling study based on a detailed gas-phase mechanism has confirmed the maturation phenomenon and its importance on one of the SL/RL transitions (from SL to RL when residence time and/or temperature increases), in the case of propane de-

composition at 2 kPa in a tubular furnace and CVD conditions²³. It appeared that only the heaviest species in the detailed model were associated to RL pyrocarbon growth, while many lighter ones were related to SL (see figures 1 and 2).

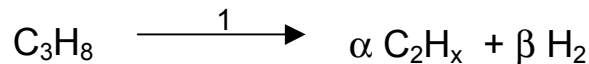
In order to bring all those results in a coherent and yet easy-to-use kinetic model, a simplified scheme will be presented for propane pyrolysis and SL/RL pyrocarbon deposition, suited to comparison with experiments of CVD and CVI for moderate to high residence times (0.1 to 10 s), low pressures (0.5 to 5 kPa), moderate temperatures (900°C to 1200°C) and propane as precursor gas. This model will be constructed from a synthesis of experimental results. Its parameters will be identified in a CVD configuration as a first guess; then, CVI results on model pores will be used to refine the parameter set and even update the whole model.

2. MODEL SETUP

The basic idea arising from experimental studies^{18,21} is a description of homogeneous maturation as a set of reactions in series, with SL and RL deposition reactions in parallel. In the case of propane as a single precursor, the following scheme has been proposed :



where *B* and *C* are two groups of gas-phase species, respectively light and heavy. From numerical computations of gas-phase pyrolysis²³, it appears that the species in group *C* would be C₁₄H₁₀ or heavier, while species in group *B* would be lighter ones, from C₂H₂ to C₆H₆. Actually, these light species, and especially the C₂H_x group, represent most of the decomposition products that are present in the gas-phase, so it is chosen to lump them together into a single species :



The value of α , β , and x have been fixed to 3/2, 1/2, and 14/3 in order to fit the actual mass and mole balances that are obtained from these computations²³. On the other hand, C₁₄H₁₀ is chosen as being representative of group *C*, so that reaction #3 reads :



However, up to this point, one essential feature of gas-phase maturation is not reproduced in such a model : as soon as propane gets decomposed, group *C* species

would appear, in contrast both with computations and experiments, and there would be RL pyrocarbon deposition occurring immediately in concurrence with SL deposition for moderate residence times. Indeed, there should be at least one non-depositing species between *B* and *C*, but this would add an extra species and make the model more difficult to use in a computational fluid dynamics (CFD) code. It has thus been decided to *model* the incubation phenomenon by turning reaction #4 non-linear, *i.e.* considering that RL pyC deposition may occur only if the partial pressure of *C* exceeds a given threshold : $R_4 = k_4[p(C) - p^*(C)]$ if $p(C) > p^*(C)$, 0 otherwise.

This completes the specification of a model frame containing maturation, and concurrent SL and RL deposition in the given set of experimental conditions. In the following, it will be intended to identify all kinetic parameters : activation energies, pre-exponential factors, and reaction orders.

3. MODEL PARAMETRIC IDENTIFICATION ON CVD CONFIGURATION

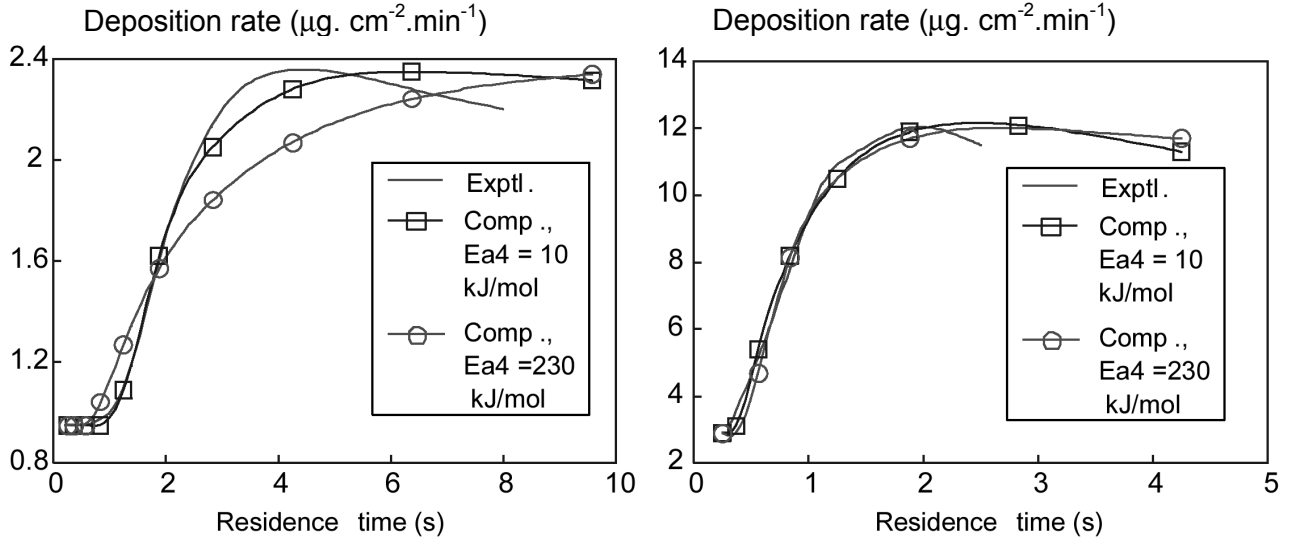
3.1. Direct identification from experimental results

The first information that may be used for parametric identification is the evolution of propane with time and temperature : actually, its decomposition is so fast that it can be considered as completely decomposed when pyC deposition begins to occur. Accordingly, no attempt is made here to give a kinetic law for reaction #1, but rather consider it as complete. Second, the heterogeneous deposition kinetics of reaction #2 may be deduced from the knowledge of the apparent kinetics in the regime where SL pyC is deposited (see figure 1). For high enough residence times, propane decomposition is indeed complete, and the reaction order is nearly zero. This can be interpreted as an adsorption-reaction scheme where the surface sites are saturated²³; consequently the order and activation energies of reaction #2 may be directly identified. As far as the next kinetic regime is concerned, the apparent order is nearly 2, with a widely varying activation energy : under the hypothesis that the homogeneous reactions are rate-limiting in this regime, this order will be affected to reaction #3. Indeed, this may be the sign of a limiting bimolecular step such as the most frequently cited ones for benzene synthesis during pyrolysis.

3.2. 1D CVD computations

The identification of the other parameters is not feasible from a direct interpretation of experimental results ; so, a 1D CVD numerical solver has been used in order to check out trial parameter sets. This solver is a simplification of a previously described one²⁴. It has turned out that various parameter sets may be chosen, with a similar correlation

quality. First, an activation energy is chosen for the heterogeneous reaction #4 ; then a pre-exponential factor for the same reaction is obtained, and the fitting procedure is ended with the determination of the two missing parameters, which are the activation energy and pre-exponential factor of reaction #3.



FIGURES 3 & 4

Comparison of deposition rates vs. residence time between experimental results and 1D CVD computations. $P = 2 \text{ kPa}$, $S/V = 118 \text{ m}^{-1}$ in hot zone , precursor : propane. $T = 950^{\circ}\text{C}$ (fig. 3), 1035°C (fig. 4)

Figures 3 and 4 show the results of the simulations with two distinct choices for $E_{a(4)}$, at the two extremes of the admissible range (10 and 230 kJ.mol^{-1}). In both cases, the fitted activation energy for reaction #3 is similar (340 and 320 kJ.mol^{-1} , respectively). So far, one degree of freedom remains : one has no indication of the actual value of the activation energy of reaction #4. We will see that model-pore CVI results help in addressing this point.

4. MODEL PARAMETRIC IDENTIFICATION ON CVI CONFIGURATION

4.1. Model-pore infiltrations

Since the precise knowledge of transport and internal surface properties is required for a CVI computation, it has been chosen to design a model porous medium built with a compact stacking of $108 \mu\text{m}$ -diameter SiC filaments, contained in a carbon crucible (figure 5). The mean pore diameter is $\approx 12 \mu\text{m}$ before deposition, a suitable value for CVI studies. It has been possible to compute all relevant transport properties in the direction parallel to the fibers, using geometrical evaluations for S/V and a previously described Monte-Carlo transport simulation software for Knudsen transport²⁵, while for binary dif-

fusion the tortuosity is known to be unity, and viscous transport is considered negligible. Figure 6 summarizes these results.

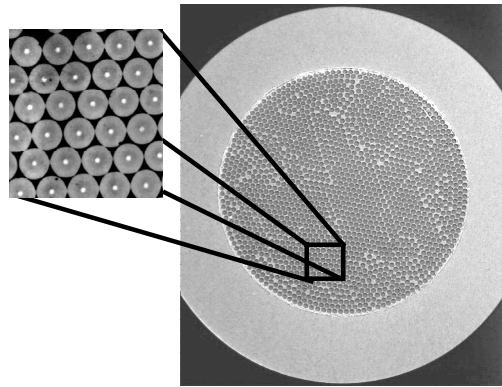


FIGURE 5
View from above of a model porous medium, with a zoomed area showing the stacking of the fibers

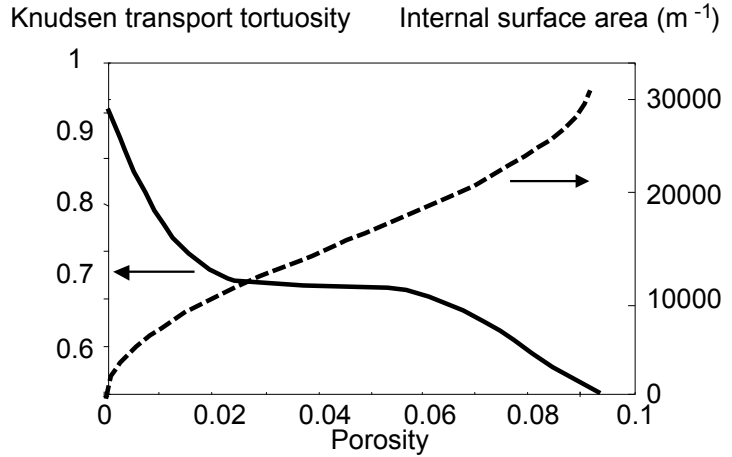


FIGURE 6
Computed laws for Knudsen transport (parallel to the fibers) and internal surface area.

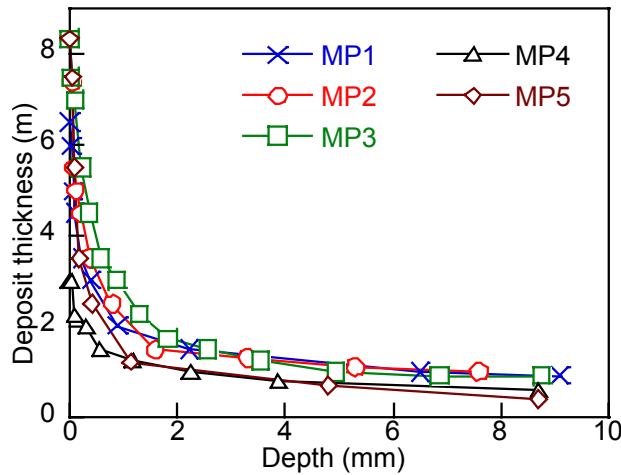


FIGURE 7
Deposit thickness profiles for 5 CVI experiments in model porous substrates.

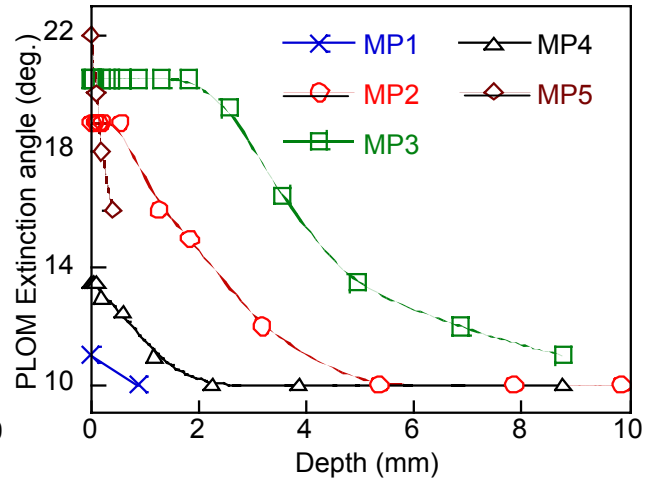


FIGURE 8
PLOM extinction angle profiles for 5 CVI experiments in model porous substrates.

Five experimental conditions have been chosen : $T = 950^{\circ}\text{C}$ with $t_s = 0.5$ s (MP1), 1.5 s (MP2) and 10 s (MP3), and $T=1035^{\circ}\text{C}$ with $t_s = 0.25$ s (MP4) and 2 s (MP5), in a way that the SL/RL transition be susceptible to appear on the deposits. The thickness profiles (figure 7) all display a sharp slope change for depths no longer than 2 mm. The values at the pore entrances were identical to the CVD values, showing that the porous medium did not interact strongly with the free-medium. The measured extinction angles in PLOM (figure 8) display a decrease, approximately at the same depth as the thickness slope break. Another striking fact is that the plateau obtained in CVD curves does

not appear in the CVI experiments (especially MP1 where it would be expected) : this would tend to invalidate the hypothesis of a Langmuir-Hinshelwood scheme, and suggest that this plateau would be the superposition of two reactions, one with an increasing rate and another with a decreasing rate, which do not depend in the same way on S/V.

4.2. Model modifications and discussion

One-dimensional CVI computations have been performed in order to reproduce the deposit thickness profiles, and particularly the slope break. An extra hypothesis has been used : the species *B* leading to SL deposition would be actually divided into two groups *B1* and *B2*, of neatly different reactivities. *B2* (and also *C* when RL is deposited) would be responsible for the rapid initial thickness decrease, the rest of the profile would be due to *B1*. Also, the idea of a zero-order deposition rate has been removed. By setting the kinetic parameters, the inlet partial pressures of the reactants appeared as a consequence of the fitting procedure. The fitted profiles were adequate when the sum of the partial pressures $p(B1) + p(B2)$ was much lower than the expected $p(B)$ from CVD experiments ; accordingly, the group *B* has been split into three contributions, *B0*, *B1* and *B2*, the species *B0* being considered as unable to yield directly any pyC deposit. Experiments MP1 and MP4 were used to obtain the deposition kinetics for SL deposition, and experiments MP2, MP3 and MP5 were used to obtain the kinetics for RL deposition and pore inlet values of $p(C)$. The latter ones have revealed to be only compatible with high values of $E_a(3)$, so the uncertainty remaining after CVD experiments has been removed. There remains only to correlate the relative amounts of *B1* and *B2* to the experimental conditions. It is to notice that *B1* has an evolution with *T* and t_s very close to C_2H_2 according to ²³, while *B2* is present in small, constant amounts whatever the experimental conditions.

The CVI model obtained is summarized in Table 1. The correlation index (residual of mean squares) has been always superior to 0,965 either in CVD or in CVI experiments.

	Balance	Pre-exp. factor A	Order	$E_a(kJ.mol^{-1})$
#1.1	$C_3H_8 \rightarrow B + 14/3 H_2$,	$1.59. 10^6 s^{-1}$	1	260
#1.1	Repartition betw. B0, B1, and B2			
#1.2	(tabulated from the C_2H_2 results of ref.[23])			
#2.1	$B1 \rightarrow 2 C(s) + 7/3 H_2$	$31.4 m.s^{-1}$	1	120
#2.2	$B2 \rightarrow 2 C(s) + 7/3 H_2$	$14148 m.s^{-1}$	1	120
#3	$7 B \rightarrow C + 34/3 H_2$	$29.9 10^{11} (mol.m^{-3})^{-0.8} s^{-1}$	1.8	320
#4	$C \rightarrow 14 C(s) + 5 H_2$	$7.10^7 m.s^{-1}$	1 w. thresh.	230
	Threshold : $p^*(C) = 119,1 - 0.21 T + 9.07 10^{-5} T^2$ (see text)			

5. TABLE 1 : Summary of the model parameters.

CONCLUSION

A first attempt to provide a complete, coherent model for both CVD and CVI of pyrocarbon from propane has been presented. It appeared that model-pore densifications brought out numerous additional informations, sometimes in apparent contradiction with CVD results. This arises essentially in the large difference in S/V ratio, and consequently of the heterogeneous-to-homogeneous reaction ratio between both. A deposit thickness slope break has led to the necessary assumption that at least two distinct species groups are responsible for SL pyC deposition, a fact that may also explain a pseudo-plateau in rate vs. residence time CVD data.

ACKNOWLEDGEMENT

The authors wish to acknowledge Snecma Moteurs for financial support.

REFERENCES

- 1) R. NASLAIN and F. LANGLAIS, *Mat. Sci. Res.* **20** (1986)145.
- 2) J. C. BOKROS, *Chemistry and Physics of Carbon* **5** (1969) 1.
- 3) P. LOLL, P. DELHAES, A. PACAULT, A. PIERRE, *Carbon*, **15** (1977) 383.
- 4) A. OBERLIN, *Carbon*, **22** (1984) 521.
- 5) R.J. DIEFENDORF, *Deposition of pyrolytic carbons*, in: *Reactivity of solids*, eds. J. W. Mitchell, R. C. de Vries, P. Cannon, Wiley & sons, New York, USA 1969.
- 6) P. LIEBERMAN and H.O. PIERSON, *Carbon*, **12** (1974) 233.
- 7) H.O. PIERSON and P. LIEBERMAN, *Carbon*, **13** (1975) 159.
- 8) K.M. SUNDARAM and G.F. FROMENT, *Chem. Eng. Sci.*, **34** (1979) 635.
- 9) R. ZOU, Q. LOU, H. LIU and F. NIU, *Ind. Eng. Chem. Res.*, **26** (1987) 2528.
- 10) L.F. ALBRIGHT and J.C. MAREK, *Ind. Eng. Chem. Res.*, **27** (1988) 755.
- 11) D.B. MURPHY and R.W. CARROLL, *Carbon*, **30** (1992) 47.
- 12) S. BAMMIDIPATI, G.D. STEWART, J. RICHARD ELLIOT Jr., S.A. GOKOGLU, and M.J. PURDY, *AIChE Journal*, **42** (1996) 3123.
- 13) C.J. CHEN and M.H. BACK, *Carbon*, **17** (1979) 175.
- 14) J.Y. LEE, J.H. JE, and H.S. KIM, *Carbon*, **21** (1983) 523.
- 15) P. LUCAS and A. MARCHAND, *Carbon*, **28** (1990) 207.
- 16) F. FAU-CANILLAC, F. CARRERE, A. REYNES, C. VALHAS and F. MAURY, *J. Phys IV France*, **5** (1995) 89.
- 17) A. BECKER and K.J. HÜTTINGER, *Carbon*, **36** (1998) 177, 201, 213 and 225.
- 18) J. LAVENAC, PhD Thesis, Université Bordeaux I, n°2274 (2000).
- 19) O. FERON, F. LANGLAIS, R. NASLAIN, and J. THEBAULT, *Carbon*, **37**(1999) 1343.
- 20) O. FERON, F. LANGLAIS, and R. NASLAIN, *Carbon*, **37** (1999) 1355.
- 21) J. LAVENAC, F. LANGLAIS, O. FERON and R. NASLAIN, *Compos. Sci. and Technol.* **61** (2001) 339.
- 22) J. LAVENAC, F. LANGLAIS, X. BOURRAT and R. NASLAIN, *J. Phys. IV France* **11** (2001) Pr3-1013.
- 23) C. DESCAMPS, G. L. VIGNOLES, O. FERON, F. LANGLAIS and J. LAVENAC, *J. de Phys. IV*, **11** (2001) Pr3-101 ; *J. Electrochem. Soc.*, **148** (2001) C695.
- 24) G.L. VIGNOLES, C. DESCAMPS and N. REUGE, *J. Phys. IV France* **10** (2000) Pr2-9
- 25) G.L. VIGNOLES, *J. Phys. IV France* **5** (1995) C5-159